

# Dynamics of Structural Elements of GB1 $\beta$ -Hairpin Revealed by Tryptophan-Cysteine Contact Formation Experiments

*Andrea Soranno<sup>1</sup>, Francesca Cabassi<sup>2</sup>, Elena Orselli<sup>2</sup>, Troy Cellmer<sup>3</sup>, Alessandro Gori<sup>4</sup>, Renato Longhi<sup>4</sup>, Marco Buscaglia<sup>2,\*</sup>*

<sup>1</sup> Department of Biochemistry and Molecular Biophysics, Washington University in St Louis, USA. <sup>2</sup> Department of Medical Biotechnology and Translational Medicine, Università degli Studi di Milano, Italy. <sup>3</sup> Laboratory of Chemical Physics, National Institute of Diabetes and Digestive and Kidney Diseases, National Institutes of Health, Bethesda, MD. <sup>4</sup> Istituto di Chimica del Riconoscimento Molecolare, Consiglio Nazionale delle Ricerche, Milano, Italy.

\* Corresponding author: [marco.buscaglia@unimi.it](mailto:marco.buscaglia@unimi.it)

**ABSTRACT** Quenching of the triplet state of tryptophan by close contact with cysteine has been shown to provide a tool for measuring the rate of intra-molecular contact formation - one of the most elementary events in the folding process - in peptides and proteins using only natural probes. Here we present a study performed on a stabilized mutant of the second  $\beta$ -hairpin of GB1 domain, where we combine steady state fluorescence, laser-induced temperature-jump, and

contact formation measurements to unveil the role of elementary structural components on hairpin dynamics and overall stability. In particular, our methodology provides access to the conformational dynamics of both the folded and unfolded state of the hairpin under native conditions, revealing the presence of extremely slow dynamics on the microsecond timescale in the unfolded state and coexistence of structures with partial pairing of the tails in the folded state. Comparing model peptides that mimic the turn sequence, we found that both ion pairing and hydrogen bonding due to the threonine side chain contribute to the propensity of turn formation, but not to the much slower dynamics of the hydrophobic core formation. Interestingly, the dynamics of the turn region in isolation are significantly faster than the dynamics measured for the unfolded state of the complete hairpin, suggesting that non-native hydrophobic contacts slow down the reconfiguration dynamics of the unfolded state. Overall, the information extracted from these experiments provides kinetic limits on interconversions among conformational populations, hence enabling to draw a simplified multi-state free-energy landscape for the GB1 hairpin.

## Introduction

Investigation of short protein fragments that adopt native-like structure in aqueous buffer have led to a better understanding of the key-factors involved in the complex process of protein folding and unfolding, helping the identification of the fundamental contacts driving structure formation and enabling the design of de-novo foldable sequences.<sup>1,2</sup> Their structural simplicity and small size have made these peptides a perfect system not only for answering fundamental questions about the early steps in the folding process, but also for practical calibration of the force fields parameter employed in molecular dynamic simulation.<sup>3,4,5,6,7</sup> Among short protein fragments retaining folding capability,<sup>8</sup>  $\beta$ -hairpins play a special role because they represent the smallest and simplest structures that in some case can undergo two-state folding in solution,

hence providing an ideal benchmark for theoretical models and atomistic molecular dynamics simulations aiming at solving the protein folding problem.<sup>9</sup> However, despite the extensive characterization of the folded structure and stability of several hairpin sequences, more detailed experimental information about the conformations and dynamics in both the folded and unfolded state would be required in order to validate the models. This challenges experimentalists to develop novel approaches and techniques to unveil hidden molecular details and provide new and different perspectives.

The C terminal  $\beta$ -hairpin of the B1 domain of the streptococcal IgG protein (GB1 in the following) has a pivotal role in this context since it has been the first sequence shown to fold independently into a  $\beta$ -hairpin structure in aqueous solution preserving a two-state behavior.<sup>10</sup> The stability of the folded structure is largely ascribed to the sequence specific turn and the hydrophobic core formed between the side chain of Val54 and the aromatic rings of Trp43, Tyr45 and Phe52. The isolated C-terminal hairpin of the GB1 has been initially characterized by Blanco et al.<sup>11,12</sup> using Nuclear Magnetic Resonance (NMR), showing that the hydrophobic cluster is preserved in the isolated structure and a significant folded fraction is present in aqueous solution in monomeric form. Despite the simple structure of the hairpin, molecular dynamics simulations have pointed out rich features, suggesting that the unfolded state of the hairpin is characterized by collapsed conformations dominated by non-native contacts.<sup>13,14,15,16</sup> On a similar trend, NMR studies have shown increasing stability in variants with mutations at the termini of the hairpin, underlining the presence of frayed ends.

The quenching of the triplet state of tryptophan by cysteine after nanosecond UV excitation has been used to measure the rate of intra-chain contact formation in unstructured peptides,

disordered proteins and folded proteins in equilibrium with their unfolded state.<sup>3,17,18,19,20,21</sup> In this approach, the long-lived triplet excited state of tryptophan is quenched by repeated contacts with an intra-chain cysteine. The analysis of the time-resolved triplet decay curves from nanoseconds to milliseconds enables to discriminate between different coexisting populations on the basis of their contact formation rates, due to either different equilibrium conformations or chain dynamics. Although many other time-resolved techniques have been proposed to access the structure and dynamics of peptides and proteins,<sup>22,23,24,25</sup> Trp-Cys contact formation is particularly advantageous in the case of small polypeptides and proteins because it does not require non-natural labeling, which can affect the statistical distribution of chain conformations.<sup>26</sup>

Here we exploit Trp-Cys contact formation to access the stability and dynamics of the three structural elements that compose a stabilized mutant of GB1  $\beta$ -hairpin: the turn region, the hydrophobic core and the tails (Figure 1a). We separately address the formation and stability of these three elements in comparison with model unstructured peptides in order to evaluate their contribution to the folding equilibrium and dynamics of the entire hairpin. To this end, we integrate the results of steady-state fluorescence intensity and fluorescence change after laser-induced temperature-jump (T-Jump) with those from contact formation between the natural tryptophan in position 45 and an engineered cysteine added to the N-terminus. Folding equilibrium, folding rate and contact formation rate were determined at different concentrations of guanidinium chloride (GdmCl), which denaturates the hairpin, and methanol (MeOH), which stabilizes the structure. We show that Trp-Cys contact formation provides access to the structural dynamics of sub-populations within the folded and unfolded states. Overall, the experimental

characterization of the accessible elementary subpopulations enables mapping the free energy landscape of the simple hairpin structure.

## Methods

**Materials.** GB1 wild-type hairpin has known to have low stability in aqueous solution. Previous studies have shown that an increase of stability can be achieved with the variant Lys41 avoiding the acetyl-amidation of the ends and mutating the Gly at the C-terminal in Glu, taking advantage of the attractive interaction between the ion pairs at the two termini.<sup>27</sup> In order to provide a probe for contact formation with the natural tryptophan at position 43, a cysteine was added at the C-terminal. A scheme of the Lys41-Glu56-Cys GB1 hairpin (GB1-KEC) is shown in Figure 1a.

The peptides studied in this work are listed in Table 1. All the peptides were synthesized by the solid-phase Fmoc method using an Applied Biosystems (Foster City, CA) peptide synthesizer. After peptide assembly, resin-bound peptides were deprotected and purified to >95% purity by semipreparative reverse-phase high-performance liquid chromatography. Peptides were prepared in aqueous solutions and in presence of different concentration of GdmCl or Methanol with 50 mM buffer potassium phosphate and adjusted to pH 6.0 to minimize disulfide formation during the preparation of the samples. In contact formation experiment, solutions were saturated with N<sub>2</sub>O to avoid the quenching of the triplet state by oxygen and to reduce the absorbance from solvated electrons. Both steady-state fluorescence and T-jump experiments were carried out with peptide concentrations of 1 μM. Tryptophan triplet quenching lifetime measurement were performed at 50 μM of peptide. A peptide with sequence GEWTY was used as a reference for fluorescence intensity of the unfolded hairpins.

**Experiments.** We used three distinct approaches to address stability, conformations, and dynamics of the  $\beta$ -hairpin peptide: a) steady-state fluorescence intensity for studying the stability of folded conformations; b) T-jump experiments for studying the folding kinetics; c) contact formation to address conformation and dynamics of unfolded or incompletely folded conformations. We performed measurements at various temperatures ( $T$ ) or concentrations of guanidinium chloride (GdmCl) and methanol (MeOH). Steady-state fluorescence intensities were acquired by a Perkin Elmer fluorescence spectrometer with excitation at 280 nm and integrating tryptophan emission between 300 nm and 450 nm. In T-jump experiments, temperature jumps of 7 K were generated by Raman shifting pulses of a Nd:YAG fundamental at 1064 nm to 1560 nm using D2 gas. To ensure a consistent T-jump in the presence of changing solvent conditions, the temperature-jump was frequently calibrated using NATA. A frequency-doubled Kr laser with an output at 284 nm was used to excite tryptophan fluorescence. Contact formation experiments were performed measuring the transient absorbance decay of tryptophan triplet state after excitation with a UV pulse.<sup>28</sup> The relatively long-lived triplet excited state is produced by means of 290 nm, 5 ns laser pulses and monitored using a diode laser at 440 nm. The reported triplet quenching rates were calculated as the mean value of three measurements, where each measure was obtained as the average decay after 256 UV pulses at 10 Hz. Given the decrease of both hairpin stability and tryptophan triplet population with temperature, the measurements were performed at 10°C in order to obtain large amplitude of the transient absorbance signal, typically in the range 6-12 mOD.

**Data analysis.** In order to extract the fraction folded  $f_f$ , steady state fluorescence intensity  $I$  was fitted using the expression  $I = (I_f - I_u)f_f + I_u$ , where  $I_u$  is the fluorescence intensity of the reference peptide GEWTY,  $I_f = c_f I_u$ , and  $c_f$  is a constant extracted from the fit. The expression of

$f_f$  is given by  $f_f = 1 - f_u$ , and  $f_u = (1 + \exp((\Delta G_0 - m[D])/RT))^{-1}$  or  $f_u = (1 + \exp(\Delta H/R(1/T - 1/T_m)))^{-1}$  for the chemical or thermal denaturation experiments, respectively, where  $[D]$  is the molar concentration of GdmCl or methanol,  $T$  is the absolute temperature and  $R$  the gas constant.

Fluorescence relaxation after T-jump was fitted by two exponentials: the fast one is due to the intrinsic change in tryptophan fluorescence with the increase of temperature; the slow one is determined by the change in hairpin population upon increasing the temperature and the quantum yield of both the folded and unfolded peptide at the final temperature. The rate  $k_{ij}$  extracted from the slower exponential is given by  $k_{ij} = k_f + k_u = k_f / f_f$ , where  $k_f$  and  $k_u$  are the kinetic rate for hairpin folding and unfolding, respectively.

To fit the tryptophan triplet decay data using the kinetic model accounting for the contact formation in the folded and unfolded states,<sup>3,18</sup>  $k_f$  and  $k_u$  were assumed to have a simple functional dependence on denaturant or methanol concentration  $[D]$  of the form  $k_f = k_{f0} \exp(m_f[D]/RT)$  and  $k_u = k_{u0} \exp(m_u[D]/RT)$ . The ratio between the folding and unfolding rates was constrained by the fraction folded,  $f_f$ , obtained from the denaturation curves measured by steady state fluorescence. Additionally, the sum of  $k_f$  and  $k_u$  and their dependence on denaturant was constrained by the relaxation rate  $k_{ij}$  measure by T-jump in aqueous buffer and at 2 M GdmCl. As described in previous works,<sup>19,20</sup> the dependence of the triplet quenching rate on the viscosity  $\eta$  was analyzed by fitting the measured decay time  $\tau_{\text{obs}}$  with  $\tau_{\text{obs}} = (qK_c)^{-1} + (\eta - A\eta^2)\tau_{0D+}$ , where  $q = 4.2 \cdot 10^9 \text{ s}^{-1}$  is the tryptophan triplet quenching rate at stable contact with cysteine,<sup>29</sup>  $K_c$  is the equilibrium constant for the population forming a Trp-Cys contact,  $\tau_{0D+}$  is the characteristic time for the first contact at the viscosity of 1 cP, and  $A$  is an empirical parameter accounting for the non-linear dependence of  $\tau_{\text{obs}}(\eta)$ .  $A$  is left as fitting parameter in the analysis of the triplet decays

within the folded and unfolded states of the GB1-KEC, whereas  $A=0$  for the analysis of model disordered peptides and turn fragments.

## Results

The description of the complex ensemble of conformations explored by a polypeptide with some structural propensity typically requires the definition of conformational basins that enable to cluster different subsets of rapidly exchanging structures.<sup>30</sup> The distinction between folded and unfolded conformations is the initial criterion to start such grouping. However, the identification of conformational basins within the folded or unfolded state of a globular protein is often challenging. In contrast, the extremely simple structure of a  $\beta$ -hairpin peptide undergoing two-state folding can greatly facilitate this task. In the case of GB1 hairpin, the folded structure coincides with the correct formation of the hydrophobic core.<sup>10</sup> As schematically shown in Figure 1b, the folded state could comprise both fully folded and partially folded structures, such as hairpins with frayed ends, whereas the unfolded state, in principle, could contain non-native conformations of the hydrophobic region, alpha-helix regions or incorrect  $\beta$ -pairing.<sup>14</sup> More generally, in the unfolded state basin we assume the presence of a heterogeneous ensemble of conformations with non-native intra-chain contacts and with no direct kinetic path to the folded state, which is accessible only through an intermediate coil-like state. In the following sections, we first address the equilibrium and kinetics of the folded and unfolded states, then we focus on the experimental characterizations and modeling of the conformational ensemble within these states, and finally we investigate the conformational propensity of the turn region.

**Hydrophobic core formation and hairpin folding.** The equilibrium characterization of the folding of GB1-KEC hairpin was performed by studying the fluorescence signal of Trp43 as a



function of temperature and solvent composition. Figure 2a shows the temperature dependence of the quantum yield in comparison with that of GB1 hairpin and that of a small peptide providing a reference of Trp43 fluorescence intensity in the unfolded state. The fluorescence increase at the lowest temperatures indicates the presence of the folded population, characterized by the hydrophobic core formed. Accordingly, the larger quantum yield of GB1-KEC hairpin indicates a larger folded population. The fraction folded of GB1-KEC (red) and GB1 hairpins (blue), calculated by fitting fluorescence steady-state measurements with a two-state population model, are reported in Figure 2b. The results are consistent with other variants of GB1 hairpin<sup>10,27</sup> and confirm the enhanced stability of GB1-KEC. At room temperature, GB1 is only 20% folded, whereas GB1-KEC shows almost a twofold increase of folded population, which reaches a fraction of about 75% at 10°C.

The fluorescence relaxation rates after laser-induced T-jump measured for the same peptides are reported in the inset of Figure 2b. The obtained values span the range 0.19 – 0.58 ( $\pm 0.05$ )  $\mu\text{s}^{-1}$  between 10°C and 30°C, similarly to what previously reported for other variants of GB1 hairpin.<sup>10</sup> Considering the fraction folded obtained from steady state fluorescence, at 10°C the corresponding folding and unfolding times are 7  $\mu\text{s}$  and 20  $\mu\text{s}$ , respectively. Since the fluorescence signal is ascribed to the change of local environment of Trp43, the folding time represents the characteristic time for forming the hydrophobic core with native structure, whereas the unfolding time corresponds to the lifetime of the hydrophobic core structure.

In order to extend the range of the observed folded population, while keeping the temperature low enough to provide a high signal for the tryptophan triplet lifetime measurements, we studied the folding equilibrium at 10°C in presence of GdmCl, acting as denaturant, and MeOH, which induces a stabilization of the hairpin structure.<sup>27,31</sup> The measured fluorescence signal and the

corresponding fraction folded are reported in Figure 3. Remarkably, the results are consistent with a single denaturation curve combining both the effect of GdmCl and MeOH. As shown in Figure 3b, a common denaturation curve is obtained assuming that an increase of the amount of MeOH from 0 to 8 M provides the same difference of folding free energy obtained decreasing the GdmCl concentration by 1 M. In this way, we were able to explore a wide range of folding fractions, from below 1% up to 98%, at constant temperature.

**Contact formation rate in the folded and unfolded state.** The presence of a tryptophan and a cysteine in the GB1-KEC hairpin enables the measurement of intra-chain contact formation by tryptophan triplet quenching. As shown in the kinetic scheme of Figure 4a, the triplet lifetime measured by nanosecond laser UV excitation depends on both the folding and unfolding rates,  $k_f$  and  $k_u$ , and on the quenching rates in the folded and unfolded state,  $k_{qf}$  and  $k_{qu}$ , respectively. The observed triplet lifetime in native (water buffer), denatured (1.5 M GdmCl) and enhanced folding (4 M MeOH) conditions is shown in Figure 4b. In all cases, the triplet lifetime is much shorter than that measured for the same peptide with the terminal cysteine inactivated by conversion into alkyl-cysteine, hence confirming that the measured decays are primarily due to tryptophan-cysteine contact formation. Overall, the measured lifetime of GB1-KEC becomes longer with the increase of folding fraction (i.e. decreasing GdmCl or increasing MeOH) but it always remains much shorter than what measured for the control peptide KEWTY. According to the kinetic model of Figure 4a, the shape of the triplet decay is given by the interplay of folding and quenching rates.<sup>3</sup> Since  $k_f$  and  $k_u$  were independently determined by the analysis of steady-state and *T*-jump fluorescence measurements, the fitting of the tryptophan triplet decay curves with the kinetic model was performed with only  $k_{qf}$  and  $k_{qu}$  as free parameters. The results, reported in Figure 5, show that, when a significant folded population is present,  $k_{qf}$  is always larger than  $k_{qu}$ .

and both rates markedly increase upon decreasing MeOH or increasing GdmCl concentrations, hence reducing the strength and lifetime of intra-chain interactions. The observed behavior of the quenching rates enables a more detailed analysis of the conformational dynamics within the folded and unfolded states, as further discussed in the following sections.

**Stability of the hairpin ends in the folded state.** The tryptophan triplet quenching rate in the folded state of GB1-KEC as a function of GdmCl and MeOH concentrations shows a continuous, monotonic decrease as the folded population increases (Figure 5). Remarkably, the trend observed at different GdmCl concentrations is perfectly consistent with that observed in MeOH. Overall, the dependence of  $k_{qf}$  is consistent with a continuous increase of free energy barrier of 0.73 kcal/mol for 1 M GdmCl reduction or for 8 M MeOH increment. The higher values of  $k_{qf}$  relative to  $k_{qu}$  indicate that in the folded state tryptophan and cysteine are more likely to form a contact. Since in the folded state the hydrophobic core is stably formed, we ascribed such large value of  $k_{qf}$  to the limited stability of the hairpin ends. In the case of a fully formed hairpin, tryptophan is not accessible to the C-terminal cysteine, whereas in the case of frayed ends cysteine can form frequent contacts with tryptophan. In the fully folded structure (Figure 1a), only two backbone hydrogen bonds are formed at the terminal region and, starting from the paired-ends conformation, Trp-Cys contact is enabled by breaking a single hydrogen bond between Lys41 and Glu56, which is stabilized by the ionic interactions between the side-chains of the same residues. Therefore, the frayed-ends state of the folded hairpin is populated by conformations with formed hydrophobic core and disordered tails, which contain no more than one backbone hydrogen bond.

In order to estimate the stability and the dynamics of the hairpin ends we measured the viscosity dependence of  $\tau_{obs} = 1/k_{qf}$  in aqueous buffer at 10°C by adding different amounts of sucrose (red

dots in Figure 6). The intercept and the slope of  $\tau_{obs}$  at low viscosity represent the reciprocal of the reaction-limited and the diffusion-limited rate for contact formation.<sup>20</sup> From this analysis, we estimated a first contact time  $\tau_{0D+} = 336$  ns and an equilibrium constant for the population forming a contact of  $K_c = 0.21 \cdot 10^{-3}$ . We compared the contact formation behavior in the folded state of GB1-KEC with that obtained for a model unstructured peptide with similar intra-chain Trp-Cys distance. Assuming a stable structure of the hydrophobic core in the folded state, the relative position of Trp43 and Val54 is fixed, hence the number of amino acids separating Trp43 and Cys57 along the virtual chain KEW-VTEC is  $3 \pm 1$ , where the uncertainty accounts for the effective W-V distance and the effective conformational freedom of Trp43 and hairpin ends. Accordingly, we chose the peptide CAQEW (AQE) as reference for the contact formation in a fully unstructured chain. Peptides with the repeated sequence AQE have been shown to behave as swollen random coils by combined FRET and Trp-Cys contact formation experiments.<sup>20</sup> Moreover, the fact that Trp43 is not at the chain terminus of the hairpin fragment is assumed to induce a limited decrease of the contact formation rate. Indeed, the addition of a tail has been shown to reduce the contact formation rate in random coil peptides only by 30% to 40%, primarily because of a decrease of accessibility to Trp-Cys contact due to excluded volume.<sup>19</sup> As shown in Figure 6, both the intercept and the slope of the triplet state lifetime  $\tau_{obs}(\eta)$  for the peptide AQE are much smaller than those of the folded state of GB1-KEC. The corresponding first contact time  $\tau_{0D+}$  and the equilibrium constant for Trp-Cys contact  $K_c$  are more than one order of magnitude smaller, as reported in Table 1. Assuming only two states for the hairpin tails in the folded state, either fully paired or fully frayed, we estimated the population and the lifetime of paired tails using AQE peptide as a model for the frayed-ends state. Accordingly, the observed quenching rate in the folded state of GB1-KEC is ascribed to the kinetic equilibrium

between the frayed-ends state, where the quenching rate is similar to the AQE peptide, and the paired-ends state, where the quenching rate is much lower. From this analysis, we obtained a fraction of folded-state population with fully paired ends of about 80% ( $\pm 5\%$ ) and a characteristic time of tail breaking of about 300 ns ( $\pm 100$  ns). Overall, these values are consistent with the values of  $K_c$ , the equilibrium constants for Trp-Cys contact formation, and of  $\tau_{0D+}$ , the first contact time, extracted for GB1-KEC and AQE (Table 1). Remarkably, the unfolding time of 20  $\mu$ s extracted from steady state and T-jump fluorescence is much longer than the lifetime of the fully paired tails, hence confirming that the hydrophobic core formation and not the tail pairing represents the structural element separating the folded and unfolded basins. However, tails pairing does contribute to the overall stability of the hairpin, as indicated by the decrease of  $k_{qf}$  with the folding fraction as a function of chemical denaturant (Figure 5).

**Conformational dynamics in the unfolded state.** The behavior of the tryptophan triplet quenching rate in the unfolded state  $k_{qu}$  shows different regimes as a function of denaturant and folding stabilizer. At GdmCl concentrations larger than 2 M, where the fraction folded is below 1%, the peptide behaves like a random coil in a good solvent. This is confirmed by the weak decrease of  $k_{qu}$  with denaturant concentration due to progressive swelling of the chain. This behavior has been previously reported for unstructured peptides,<sup>19,20</sup> as well as for the unfolded state of globular proteins.<sup>17,18,32</sup> Remarkably, decreasing the concentrations of GdmCl from 1.5 M to 0 M,  $k_{qu}$  progressively decreases and maintains this trend also upon further increase of the folded fraction by adding MeOH. A similar decrease of the contact formation rate in the unfolded state close to native conditions was previously observed only in much larger globular proteins.<sup>33,34</sup> The increase of the number and strength of inter-residue interactions expected upon decreasing the concentration of denaturant can lead to a reduction of both the volume explored

by the chain and the intra-chain dynamics. However, these two mechanisms have opposite effects on the observed contact formation rate. Accordingly, the reduction of  $k_{qu}$  at increasing the folding fraction is ascribed to a strong reduction of conformational dynamics, possibly in combination with a weaker opposite effect due compaction. In order to confirm this hypothesis, we measured the viscosity dependence of  $k_{qu}$  repeating the fitting of the kinetic model of Figure 4a to triplet decay curves obtained at different concentration of sucrose. The measured dependence of the observed time  $k_{qu}^{-1}$  for the GB1-KEC peptide is reported in Figure 6 (blue dots). The figure also shows the tryptophan triplet quenching time previously measured for a model unstructured peptide with similar length, AQE4.<sup>20</sup> The steeper viscosity dependence of GB1-KEC indicates a larger value of the diffusion-limited contact formation time,  $\tau_{D+}$ , which represents the time of the first tryptophan-cysteine contact after UV excitation. From the fit of GB1-KEC data, we obtained  $\tau_{D+} = 3 \mu s$ , and  $K_c = 0.1 \cdot 10^{-3}$  (Table 1), corresponding to an intra-chain dynamics about 20 times slower than that of AQE4 and also a smaller fraction of equilibrium conformation with Trp-Cys contact, respectively. These results suggest that the unfolded state of GB1-KEC is characterized by rather strong inter-residue non-native interactions that reduce the chain conformational dynamics, and hence the Trp-Cys contact.

**Turn formation propensity in the unfolded state.** The turn region of the hairpin plays a major role in the folding process because the formation of the correct turn structure is essential for the native pairing of all other residues,<sup>15</sup> even when assuming different folding processes such as the nucleation of a hydrophobic core or the consecutive zipping of native contacts. Moreover, the turn formation involves only local intra-chain interactions, hence, in principle, it can be faster than the other structural elements of the hairpin. In order to investigate the conformational propensity of the GB1-KEC turn region, we studied the end-to-end contact formation rate of the

turn fragment terminated with a tryptophan and a cysteine. In this case, the formation of a Trp-Cys contact in the truncated peptides does not represent a model for the formation of the well-structured turn in the full-length hairpin, which is also affected by the reduced chain dynamics of the unfolded state under native conditions. Nevertheless, given the short length of the turn fragments, the Trp-Cys contact rate is assumed as a measure of the local sequence propensity to adopt conformations most similar to the turn structure. We compared the native sequence (peptide DT in table 1) with three other variants obtained removing either the attractive ion pairing between aspartic acid and lysine (peptide NT) or the hydrogen bonds due to threonine residues (peptide DX) or both (peptide NX). In addition, we also compared the behavior of these peptides to that of disordered peptides assumed as model for a swollen chain (peptide AQEAQQ) or for a glycine-rich chain with balanced repulsive and attractive interaction (peptide AGQ2).<sup>19</sup> The measured triplet decay curves in aqueous buffer at 10°C are reported in Figure 7a and the viscosity dependence of the corresponding triplet lifetime is shown in Figure 7b. Remarkably, all four variants of the turn fragments have a fraction of population with Trp-Cys contact at equilibrium between that of AGQ2 and AQEAQQ, as indicated by the values of  $K_c$  in Table 1. Moreover, the native fragment presents the largest population with end-to-end contact among the turn variants. This confirms that the native sequence has a turn propensity compatible with the presence of attractive inter-residue interactions provided by both ion pairing and hydrogen bonds. In particular, the hydrogen bonds due to threonine showed the largest contribution to the turn propensity, as suggested by the larger decrease of  $K_c$  for peptides DX and NX. The study of the viscosity dependence also enabled to estimate the characteristic time for the first Trp-Cys contact. For all the variants, the extracted time  $\tau_{0D+}$  is in the range 65-75 ns, hence much faster than the time required for the correct formation of the hydrophobic core, which corresponds to

the folding time. This confirms that the turn formation is not the rate-limiting step for the hairpin folding, although its amino acid sequence is optimized for a large structural turn propensity.

## Discussion

The combination of laser T-jump and contact formation experiments provides new insights on the population and dynamics of the main conformational basins of the GB1-KEC and enables to draw a model-free draft of the  $\beta$ -hairpin free-energy landscape accounting for sub-populations within the folded and unfolded basins (Figure 8). The slowest process is associated with the free-energy barrier separating the unfolded and the folded state, which is identified as in previous works by the formation of the hydrophobic core. Interestingly, contact formation experiments suggest the presence of other barriers within these two basins. In the folded basin, the hairpin ends are not stably paired and undergo a continuous exchange between a stabilized conformation (in which the Trp-Cys contact is inhibited) and a frayed-ends conformation (in which there is rapid quenching of the tryptophan triplet). Given the small size of the terminal region, the highly dynamic frayed-ends state is consistent with negligible transient intra-chain interactions between the tails, hence resembling the behavior of a disordered peptide fragment. Accordingly, the viscosity dependence of the triplet lifetime decays (Figure 6) is quantitatively compared to that of the model peptide AQE (Table 1), hence obtaining that the stabilized conformation with fully-paired ends is more abundant than the fraction with frayed-ends. Moreover, as shown in Figure 5, the triplet quenching rate in the folded state decreases with the increase of the hairpin stability as a function of GmdCl and MeOH, similarly to the overall unfolding rate of the hairpin. This suggests a strong correlation between the lifetime of the paired ends conformation and the unfolding time. Accordingly, in the free energy landscape, the frayed-ends basin represents a low populated intermediate between the transition state for folding and the fully folded conformation



with fully paired ends, as reported in previous works.<sup>27,35</sup> Remarkably, the presence of two free-energy minima in the folded state of GB1-KEC mutant is also predicted by the simple Ising-like model proposed by Muñoz and Eaton<sup>10,36,37,38</sup> (Figure S1). Relative to the wild type peptide GB1, the interaction between Lys and Glu added to the hairpin tails induces an enthalpy increase of  $\Delta H_{KE} = 1.76$  kcal/mol that shifts the global minimum of free-energy to the formation of 15 native contacts (fully-paired ends), and leaving a secondary minimum at 11 contacts (frayed ends).

For what concerns the unfolded basin, the Trp-Cys contact formation experiments indicate the presence of conformations that are exchanging very slowly on the microsecond timescale. In contrast, the analysis of the turn peptides suggests that the hairpin sequence encodes chain conformational dynamics with frequent closure of the turn loop that brings in contact the first hydrophobic residues of the core (Y45 and F52). Interestingly, these events occur on a time scale much faster than the time observed for the dynamics of the unfolded state of the complete hairpin peptide, with a characteristic contact formation time of the turn of about 75 ns. A more direct comparison can be obtained using the Szabo-Schulten-Schulten (SSS) theory for diffusion-limited contact formation<sup>39</sup> and rescaling the contact formation time of the turn to the one of the complete hairpin. In this respect, peptides with the repeated sequence Ala-Gly-Gln have been shown to behave like an ideal chain with negligible non-local inter-residue interactions in aqueous buffer, hence they provide an experimental reference for the expected behavior of a random coil.<sup>19,40</sup> The first contact time of an ideal sequence similar to GB1-KEC at 10°C can be estimated considering a Trp-Cys distance of 13 aa and a 30% increase due to the fact that Trp is not at the chain. Assuming the same dependence of the Ala-Gly-Gln series, this would lead to  $\tau_{0d+}$  smaller than 100 ns. However, it has been shown that soluble unstructured proteins and peptides typically behave like swollen polymers, due to predominant inter-residue repulsive

interactions ascribed to either net charge or excluded volume.<sup>41</sup> Analogously, a model peptide for contact formation in a swollen chain is given by the repeated sequence Ala-Gln-Glu.<sup>20</sup> Also in this case, the value of  $\tau_{0d+} \approx 250$  ns extrapolated for a sequence similar to GB1-KEC is much faster than the hairpin value.

The slow dynamics of the unfolded state of GB1-KEC under native conditions is consistent with recent measurements of internal friction effects in the unfolded state of proteins,<sup>33,42,43,44,45,46</sup> in particular with contact formation experiments that probed the dynamics of short segments (comprising a similar number of amino acids) with protein L and acyl-coenzyme A binding protein.

Recent experiments and simulations suggest that such slowdown of dynamics in the disordered state may originate from different contributions: i) dihedral angle rotations and crankshaft motions; ii) non-native hydrophobic or salt bridge interactions; iii) hydrogen bond formation. In this respect, the observation of internal friction effects in a small peptide such as the GB1 hairpin enables us to estimate the contribution of these different elements. Let's consider first the effect of dihedral angles and crankshaft motions. This has been well understood in terms of the so-called Kuhn theorem, which states that with increasing length of the chain the contribution of dihedral rotations to internal friction decreases until becoming negligible when compared to chain dynamics. In this respect, the slower dynamics of the full-length hairpin when compared to the turn suggests that dihedral angles have a minor contribution to the contact formation time ( $\leq 75$  ns). Let's consider the contribution of non-native contacts. The GB1-KEC sequence contains only 2 positively charged residues (K41 and K50) that in the folded structure are found to form salt bridges at the termini and in the turn, respectively. Interestingly, point mutations of the charged residues in the turn do not significantly alter the dynamics of the turn (see DT, TX, NT,

NX constructs in Table 1), suggesting that the contribution of charged interactions is negligible. A similar conclusion is obtained also by comparing the contact formation dynamics of frayed ends with the ones obtained for disordered peptides of similar length (see AGQ2, AQEAQQ, in Table 1). Therefore, attractive electrostatics interactions appear to have a small effect, although measurable, on contact formation dynamics. Consequently, the origin of the microsecond slow dynamics in the unfolded state can be restricted to the remaining two factors, i.e. the formation of non-native hydrophobic contacts or the formation of non-native hydrogen bonds. An analogous argument to the one of charged residues can be used for the formation of long-range hydrogen bonds, since their contribution to the turn and frayed-ends dynamics is mostly negligible (even though, we cannot exclude incremental effects due to the formation of multiple non-native long-range hydrogen bonds). All the information points to a critical contribution of the hydrophobic residues that constitutes the core of the folded hairpin. Indeed, formation of “misfolded” states with incorrect contacts between the aromatic residues of the hydrophobic core has been observed within the unfolded basin in MD simulations.<sup>15,16</sup>

The slow dynamics observed in the unfolded state poses an interesting question on the elementary steps controlling folding. Indeed, contact formation of the hydrophobic residues is the elementary step of folding for the GB1  $\beta$ -hairpin. Interestingly the end-to-end contact formation of the turn fragments in isolation is much faster than the chain dynamics in the unfolded state of the complete hairpin, suggesting that internal friction dominates the rate-limiting step of folding. This is not surprising if interpreted as the formation of long-lived incorrect contacts between the same aromatic residues that constitute the core of the folded conformation. In this respect, internal friction would represent for the GB1 hairpin non-productive attempts of forming the correct hydrophobic core.

## Conclusions

We studied the folding of a  $\beta$ -hairpin peptide by combining steady-state fluorescence laser temperature-jump and contact formation experiments. The analysis of the results as a function of temperature, chemical denaturant, stabilizing agent, and viscosity as well as the comparison with model unstructured peptides enable an experimental characterization of the multiple conformational basins of the  $\beta$ -hairpin. We identified the role played by the three main structural elements, namely the turn, the hydrophobic core and the tails, in the folding/unfolding equilibrium of the hairpin. Although the formation of the hydrophobic core represents the limiting factor for folding, the ionic and hydrogen bond interactions encoded in the peptide sequence play a major role on the turn propensity and the tail stabilization, hence on the overall hairpin equilibrium and dynamics. In this respect, the lifetime of tails pairing is found to correlate with the stability of the folded state as a function of GdmCl and MeOH. In contrast, the search for the native hydrophobic core structure in the unfolded state is affected by the structural propensity of the turn region, which influences the probability of forming the contact but only marginally the dynamics, and by the strength of the inter-residue interactions, which strongly reduces the conformational dynamics of the unfolded state in native conditions and provides a major limitation to the folding time.

## FIGURES

**Figure 1.** Folded structure of GB1-KEC  $\beta$ -hairpin and schematic representation of possible conformational states. (a) The structure is composed by three parts: the turn region, the hydrophobic core, and the terminal tails. Hydrophobic, positively charged or negatively charged residues are indicated in green, red and blue, respectively. The main hydrogen bonds holding the hairpin structure are indicated by green dotted lines. (b) Tryptophan fluorescence, either steady-state or after laser-induced T-jump, probes the formation of the hydrophobic core. In contrast, tryptophan triplet lifetime probes the contact formation with cysteine. The folded state is identified by the formation of the native structure of the central hydrophobic core (represented as a cross in the scheme). Within the folded state, populations with well-formed and partially-formed tail pairing are expected. Transient non-native contacts are expected in the unfolded state, whereas a random coil behavior corresponds to a negligible number of attractive contacts.

**Figure 2.** Folded fraction of  $\beta$ -hairpins as a function of temperature. (a) Temperature dependence of steady-state fluorescence quantum yield of Trp43 measured for an excitation at 280 nm for the GB1-KEC (red) and GB1 hairpins (blue) and for the reference GEWTY peptide (magenta) in aqueous solution. Absolute values of quantum yields are calculated in comparison with a sample of NATA. The quantum yield of the folded state (green dash line) has been obtained multiplying the curve of the unfolded state by a constant  $c_f = 1.7$ , in order to reproduce the amplitudes of the T-jump measurements. (b) Fraction folded of GB1-KEC (red) and GB1 hairpins (blue) obtained from fluorescence steady-state measurements. Inset: relaxation rates measured by T-jump experiments for GB1-KEC in aqueous buffer (red) and in 2 M GdmCl (green), and for GB1 in aqueous buffer (blue).

**Figure 3.** Folded fraction of GB1-KEC  $\beta$ -hairpin as a function of chemical denaturant and stabilizer. Dependence of the steady-state fluorescence intensity measured for the hairpin (red) as a function of the concentration of MeOH (a) and GdmCl (b). The fluorescence of GEWTY peptide is assumed as the signal of the unfolded state (magenta), whereas the folded state fluorescence (green dashed line) is obtained from the same curve multiplied by a constant  $c_f$ , coherently with the analysis of temperature unfolding data (Figure 2). (c) Fraction folded as a function of MeOH and GdmCl obtained from fluorescence measurements. The scale reporting MeOH concentration has been compressed in order to match the different dependence of the hairpin free-energy on MeOH and GdmCl obtained from the analysis of fluorescence intensity (panel a and b).

**Figure 4.** Tryptophan triplet quenching by contact formation with cysteine in GB1-KEC. (a) Kinetic model combining hairpin folding and unfolding with triplet quenching. The time-resolved triplet decay curves after UV excitation depend on the rates for folding ( $k_f$ ) and unfolding ( $k_u$ ), as well as on the quenching rates in folded ( $k_{qf}$ ) and unfolded ( $k_{qu}$ ) states. (b) Transient absorbance at 440 nm indicating the hairpin population with excited triplet state for GB1-KEC in aqueous buffer (green), 1.5 M GdmCl (blue), 4 M MeOH, and corresponding fits (black lines) obtained by the kinetic model. The same peptide after inactivation of the cysteine quenching by conversion into alkyl-cysteine provides a much longer decay time (gray) fitted by a single exponential decay (black lines).

**Figure 5.** Tryptophan triplet quenching rates of GB1-KEC as a function of GdmCl and MeOH. The triplet quenching rate  $k_{qf}$  (red dots) and  $k_{qu}$  (blue dots) are obtained from the fit of the triplet decay curves with the kinetic model reported in Figure 4a. The black dashed line fitting the red dots is obtained as  $k_{qf} = k_{qf0} \exp(E_f[D])$ , where  $k_{qf0} = 5.5 \cdot 10^5 \text{ s}^{-1}$ ,  $E_f = 1.29 \text{ M}^{-1}$  and  $[D]$  is the

molar concentration of GdmCl or the molar concentration of MeOH multiplied by -0.125. The blue dots for GdmCl concentrations larger than 1.5 M are fitted with  $k_{qu} = k_{qu0} \exp(E_u[D])$ , where  $k_{qu0} = 6.5 \cdot 10^5 \text{ s}^{-1}$ ,  $E_u = -0.096 \text{ M}^{-1}$ . black dashed line on top of the blue dots is a polynomial fit to guide the eye. The dashed red and blue lines represent the rate for folding ( $k_f$ ) and unfolding ( $k_u$ ), respectively.

**Figure 6.** Trp-Cys contact formation in GB1-KEC hairpin and model unstructured peptides. Triplet decay time constants as a function of viscosity measured for the folded and unfolded states of GB1-KEC, as  $\tau_{obs} = 1/k_{qf}$  (red full dots and line) and  $\tau_{obs} = 1/k_{qu}$  (blue dots and line), respectively, and for peptides AQE4 (blue dashed line) and AQE (red open dots and dashed line). The sample viscosity has been changed adding sucrose up to 40% w/w. The data for AQE4 are obtained from reference <sup>20</sup>. Inset: enlarged view of the low viscosity region.

**Figure 7.** Trp-Cys contact formation for turn peptides. (a) Transient absorbance for peptides DT (red), DX (purple), NT (magenta), NX (orange), AGQ (green) and AQE (blue). The black lines represent fits with single exponential decays. (b) Triplet decay lifetime measured as a function of viscosity (dots) and linear fits (lines). The color code is the same of panel a.

**Figure 8.** Free-energy landscape of GB1-KEC  $\beta$ -hairpin. Schematic representation of the free-energy minima and barriers associated to the different conformations of the hairpin peptide. The barrier heights indicated by the horizontal segments are obtained by experimental determination of contact formation kinetics.

# TABLES

**Table 1.** Peptides studied by Trp-Cys contact formation and extracted parameters.

| Name              | Sequence                                                            | Cys-Trp<br>distance (aa) | Conformation      | Cys-Trp contact formation |                     |                       |
|-------------------|---------------------------------------------------------------------|--------------------------|-------------------|---------------------------|---------------------|-----------------------|
|                   |                                                                     |                          |                   | $\tau_{obs}$ ( $\mu$ s)   | $K_c$ ( $10^{-3}$ ) | $\tau_{\infty+}$ (ns) |
| GB1-KEC           | ADDYTWEEK+                                                          | 13                       | Folded            | 1.6                       | 0.21                | 336                   |
|                   | TKTFTVTEC-                                                          |                          | Unfolded          | 5.9                       | 0.10                | 3000                  |
| DT                | ADD <sup>C</sup> -Ac<br> <br>TKT <sup>W</sup> -NH <sub>2</sub>      | 6                        | Disordered / turn | 0.30                      | 1.14                | 75                    |
| DX                | ADD <sup>C</sup> -Ac<br> <br>XKX <sup>W</sup> -NH <sub>2</sub>      | 6                        | Disordered / turn | 0.55                      | 0.59                | 77                    |
| NT                | ANN <sup>C</sup> -Ac<br> <br>TKT <sup>W</sup> -NH <sub>2</sub>      | 6                        | Disordered / turn | 0.38                      | 0.74                | 73                    |
| NX                | ANN <sup>C</sup> -Ac<br> <br>XKX <sup>W</sup> -NH <sub>2</sub>      | 6                        | Disordered / turn | 0.47                      | 0.60                | 65                    |
| AQE               | Ac-C <sup>A</sup> Q <sup>E</sup> W-NH <sub>2</sub>                  | 3                        | Disordered        | 0.24                      | 1.2                 | 26                    |
| AGQ2 <sup>a</sup> | Ac-C <sup>A</sup> GQAGQ <sup>W</sup> -NH <sub>2</sub>               | 6                        | Disordered        | 0.16                      | 2.1                 | 58                    |
| AQEAQQ            | Ac-C <sup>A</sup> Q <sup>E</sup> AQQ <sup>W</sup> -NH <sub>2</sub>  | 6                        | Disordered        | 0.74                      | 0.36                | 93                    |
| AQE4 <sup>b</sup> | Ac-C <sup>A</sup> (AQ <sup>E</sup> ) <sub>4</sub> W-NH <sub>2</sub> | 12                       | Disordered        | 0.98                      | 0.31                | 170                   |

<sup>a</sup> Data from ref. 19. <sup>b</sup> Data from ref. 20.



## AUTHOR INFORMATION

### **Corresponding Author**

\* marco.buscaglia@unimi.it

### **Author Contributions**

The manuscript was written through contributions of all authors. All authors have given approval to the final version of the manuscript.

## SUPPORTING INFORMATION

Calculation of the free-energy profile of GB1-KEC  $\beta$ -hairpin by Muñoz-Eaton model.

Distribution of Trp-Cys distances of the unfolded GB1-KEC peptide with only excluded volume interactions computed by CBX model.

## ACKNOWLEDGMENT

We thank William A. Eaton and James Hofrichter for helpful discussion. This work was supported by Regione Lombardia (Ingenio 2007).

## REFERENCES

- (1) Singhal, N.; Snow, C. D.; Pande, V. S. Using Path Sampling to Build Better Markovian State Models: Predicting the Folding Rate and Mechanism of a Tryptophan Zipper Beta Hairpin. *J. Chem. Phys.* **2004**, *121* (1), 415.
- (2) Lacroix, E.; Kortemme, T.; Delapaz, M.; Serrano, L. The Design of Linear Peptides That Fold as Monomeric  $\beta$ -Sheet Structures. *Curr. Opin. Struct. Biol.* **1999**, *9* (4), 487–493.
- (3) Cellmer, T.; Buscaglia, M.; Henry, E. R.; Hofrichter, J.; Eaton, W. A. Making Connections between Ultrafast Protein Folding Kinetics and Molecular Dynamics Simulations. *Proc. Natl. Acad. Sci.* **2011**, *108* (15), 6103–6108.
- (4) Mittal, J.; Best, R. B. Tackling Force-Field Bias in Protein Folding Simulations: Folding of Villin HP35 and Pin WW Domains in Explicit Water. *Biophys. J.* **2010**, *99* (3), L26–L28.
- (5) Cino, E. A.; Choy, W.-Y.; Karttunen, M. Comparison of Secondary Structure Formation Using 10 Different Force Fields in Microsecond Molecular Dynamics Simulations. *J. Chem. Theory Comput.* **2012**, *8* (8), 2725–2740.
- (6) Best, R. B.; Zheng, W.; Mittal, J. Balanced Protein–Water Interactions Improve Properties of Disordered Proteins and Non-Specific Protein Association. *J. Chem. Theory Comput.* **2014**, *10* (11), 5113–5124.
- (7) Piana, S.; Lindorff-Larsen, K.; Shaw, D. E. How Robust Are Protein Folding Simulations with Respect to Force Field Parameterization? *Biophys. J.* **2011**, *100* (9), L47–L49.

- (8) Kubelka, J.; Hofrichter, J.; Eaton, W. A. The Protein Folding ‘Speed Limit.’ *Curr. Opin. Struct. Biol.* **2004**, *14* (1), 76–88.
- (9) Dill, K. A.; Ozkan, S. B.; Shell, M. S.; Weikl, T. R. The Protein Folding Problem. *Annu. Rev. Biophys.* **2008**, *37* (1), 289–316.
- (10) Muñoz, V.; Thompson, P. A.; Hofrichter, J.; Eaton, W. A. Folding Dynamics and Mechanism of  $\beta$ -Hairpin Formation. *Nature* **1997**, *390* (6656), 196–199.
- (11) Blanco, F. J.; Jimenez, M. A.; Herranz, J.; Rico, M.; Santoro, J.; Nieto, J. L. NMR Evidence of a Short Linear Peptide That Folds into a  $\beta$ -Hairpin in Aqueous Solution. *J. Am. Chem. Soc.* **1993**, *115* (13), 5887–5888.
- (12) Blanco, F. J.; Rivas, G.; Serrano, L. A Short Linear Peptide That Folds into a Native Stable  $\beta$ -Hairpin in Aqueous Solution. *Nat. Struct. Mol. Biol.* **1994**, *1* (9), 584–590.
- (13) Best, R. B.; Mittal, J. Free-Energy Landscape of the GB1 Hairpin in All-Atom Explicit Solvent Simulations with Different Force Fields: Similarities and Differences. *Proteins Struct. Funct. Bioinforma.* **2011**, *79* (4), 1318–1328.
- (14) De Sancho, D.; Mittal, J.; Best, R. B. Folding Kinetics and Unfolded State Dynamics of the GB1 Hairpin from Molecular Simulation. *J. Chem. Theory Comput.* **2013**, *9* (3), 1743–1753.
- (15) Best, R. B.; Mittal, J. Microscopic Events in  $\beta$ -Hairpin Folding from Alternative Unfolded Ensembles. *Proc. Natl. Acad. Sci.* **2011**, *108* (27), 11087–11092.
- (16) Bonomi, M.; Branduardi, D.; Gervasio, F. L.; Parrinello, M. The Unfolded Ensemble and

- Folding Mechanism of the C-Terminal GB1 -Hairpin. *J. Am. Chem. Soc.* **2008**, No. 31, 13938–13944.
- (17) Buscaglia, M.; Schuler, B.; Lapidus, L. J.; Eaton, W. A.; Hofrichter, J. Kinetics of Intramolecular Contact Formation in a Denatured Protein. *J. Mol. Biol.* **2003**, 332 (1), 9–12.
- (18) Buscaglia, M.; Kubelka, J.; Eaton, W. A.; Hofrichter, J. Determination of Ultrafast Protein Folding Rates from Loop Formation Dynamics. *J. Mol. Biol.* **2005**, 347 (3), 657–664.
- (19) Buscaglia, M.; Lapidus, L. J.; Eaton, W. a; Hofrichter, J. Effects of Denaturants on the Dynamics of Loop Formation in Polypeptides. *Biophys. J.* **2006**, 91 (1), 276–288.
- (20) Soranno, A.; Longhi, R.; Bellini, T.; Buscaglia, M. Kinetics of Contact Formation and End-to-End Distance Distributions of Swollen Disordered Peptides. *Biophys. J.* **2009**, 96 (4), 1515–1528.
- (21) Sizemore, S. M.; Cope, S. M.; Roy, A.; Ghirlanda, G.; Vaiana, S. M. Slow Internal Dynamics and Charge Expansion in the Disordered Protein CGRP: A Comparison with Amylin. *Biophys. J.* **2015**, 109 (5), 1038–1048.
- (22) Fierz, B.; Satzger, H.; Root, C.; Gilch, P.; Zinth, W.; Kiefhaber, T. Loop Formation in Unfolded Polypeptide Chains on the Picoseconds to Microseconds Time Scale. *Proc. Natl. Acad. Sci.* **2007**, 104 (7), 2163–2168.
- (23) Nettels, D.; Gopich, I. V; Hoffmann, A.; Schuler, B. Ultrafast Dynamics of Protein Collapse from Single-Molecule Photon Statistics. *Proc. Natl. Acad. Sci. USA* **2007**, 104,

2655–2660.

- (24) Huang, F.; Hudgins, R. R.; Nau, W. M. Primary and Secondary Structure Dependence of Peptide Exhibility Assessed by Uorescence-Based Measurement of End-to-End Collision Rates. *J. Am. Chem. Soc* **2004**, *126*, 16665–16675.
- (25) Neuweiler, H.; Doose, S.; Sauer, M. A Microscopic View of Miniprotein Folding: Enhanced Folding Efficiency through Formation of an Intermediate. *Proc. Natl. Acad. Sci. U. S. A.* **2005**, *102* (46), 16650–16655.
- (26) Borgia, A.; Borgia, M. B.; Bugge, K.; Kissling, V. M.; Heidarsson, P. O.; Fernandes, C. B.; Sottini, A.; Soranno, A.; Buholzer, K. J.; Nettels, D.; et al. Extreme Disorder in an Ultrahigh-Affinity Protein Complex. *Nature* **2018**, *555* (7694), 61–66.
- (27) Huyghues-Despointes, B. M. P.; Qu, X.; Tsai, J.; Scholtz, J. M. Terminal Ion Pairs Stabilize the Second  $\beta$ -Hairpin of the B1 Domain of Protein G. *Proteins Struct. Funct. Bioinforma.* **2006**, *63* (4), 1005–1017.
- (28) Lapidus, L. J.; Eaton, W. A.; Hofrichter, J. Measuring the Rate of Intramolecular Contact Formation in Polypeptides. *Proc. Natl. Acad. Sci.* **2000**, *97* (13), 7220–7225.
- (29) Lapidus, L.; Eaton, W.; Hofrichter, J. Dynamics of Intramolecular Contact Formation in Polypeptides: Distance Dependence of Quenching Rates in a Room-Temperature Glass. *Phys. Rev. Lett.* **2001**, *87* (25), 258101.
- (30) Lindorff-Larsen, K.; Piana, S.; Dror, R. O.; Shaw, D. E. How Fast-Folding Proteins Fold. *Science* **2011**, *334* (6055), 517–520.

- (31) Searle, M. S.; Zerella, R.; Williams, D. H.; Packman, L. C. Native-like  $\beta$ -Hairpin Structure in an Isolated Fragment from Ferredoxin: NMR and CD Studies of Solvent Effects on the N-Terminal 20 Residues. *Protein Eng. Des. Sel.* **1996**, *9* (7), 559–565.
- (32) Schuler, B.; Lipman, E. A.; Eaton, W. A. Probing the Free-Energy Surface for Protein Folding with Single-Molecule Fluorescence Spectroscopy. *Nature* **2002**, *419* (6908), 743–747.
- (33) Waldauer, S. A.; Bakajin, O.; Lapidus, L. J. Extremely Slow Intramolecular Diffusion in Unfolded Protein L. *Proc. Natl. Acad. Sci.* **2010**, *107* (31), 13713–13717.
- (34) Voelz, V. A.; Singh, V. R.; Wedemeyer, W. J.; Lapidus, L. J.; Pande, V. S. Unfolded-State Dynamics and Structure of Protein L Characterized by Simulation and Experiment. *J. Am. Chem. Soc.* **2010**, *132* (13), 4702–4709.
- (35) Olsen, K. A.; Fesinmeyer, R. M.; Stewart, J. M.; Andersen, N. H. Hairpin Folding Rates Reflect Mutations within and Remote from the Turn Region. *Proc. Natl. Acad. Sci.* **2005**, *102* (43), 15483–15487.
- (36) Munoz, V.; Henry, E. R.; Hofrichter, J.; Eaton, W. A. A Statistical Mechanical Model for  $\beta$ -Hairpin Kinetics. *Proc. Natl. Acad. Sci.* **1998**, *95* (11), 5872–5879.
- (37) Munoz, V.; Eaton, W. A. A Simple Model for Calculating the Kinetics of Protein Folding from Three-Dimensional Structures. *Proc. Natl. Acad. Sci.* **1999**, *96* (20), 11311–11316.
- (38) Bruscolini, P.; Pelizzola, A. Exact Solution of the Muñoz-Eaton Model for Protein Folding. *Phys. Rev. Lett.* **2002**, *88* (25), 258101.

- (39) Szabo, A.; Schulten, K.; Schulten, Z. First Passage Time Approach to Diffusion Controlled Reactions. *J. Chem. Phys.* **1980**, *72* (8), 4350–4357.
- (40) Yeh, I.-C.; Hummer, G. Peptide Loop-Closure Kinetics from Microsecond Molecular Dynamics Simulations in Explicit Solvent. *J. Am. Chem. Soc.* **2002**, *124* (23), 6563–6568.
- (41) Soranno, A.; Buchli, B.; Nettels, D.; Cheng, R. R.; Muller-Spath, S.; Pfeil, S. H.; Hoffmann, A.; Lipman, E. A.; Makarov, D. E.; Schuler, B. Quantifying Internal Friction in Unfolded and Intrinsically Disordered Proteins with Single-Molecule Spectroscopy. *Proc. Natl. Acad. Sci.* **2012**, *109* (44), 17800–17806.
- (42) Voelz, V. A.; Jäger, M.; Yao, S.; Chen, Y.; Zhu, L.; Waldauer, S. A.; Bowman, G. R.; Friedrichs, M.; Bakajin, O.; Lapidus, L. J.; et al. Slow Unfolded-State Structuring in Acyl-CoA Binding Protein Folding Revealed by Simulation and Experiment. *J. Am. Chem. Soc.* **2012**, *134* (30), 12565–12577.
- (43) Cheng, R. R.; Hawk, A. T.; Makarov, D. E. Exploring the Role of Internal Friction in the Dynamics of Unfolded Proteins Using Simple Polymer Models. *J. Chem. Phys.* **2013**, *138* (7), 074112.
- (44) Soranno, A.; Holla, A.; Dingfelder, F.; Nettels, D.; Makarov, D. E.; Schuler, B. Integrated View of Internal Friction in Unfolded Proteins from Single-Molecule FRET, Contact Quenching, Theory, and Simulations. *Proc. Natl. Acad. Sci.* **2017**, *114* (10), E1833–E1839.
- (45) Soranno, A.; Zosel, F.; Hofmann, H. Internal Friction in an Intrinsically Disordered Protein—Comparing Rouse-like Models with Experiments. *J. Chem. Phys.* **2018**, *148*

(12), 123326.

- (46) Chung, H. S.; Piana-Agostinetti, S.; Shaw, D. E.; Eaton, W. A. Structural Origin of Slow Diffusion in Protein Folding. *Science* **2015**, *349* (6255), 1504–1510.



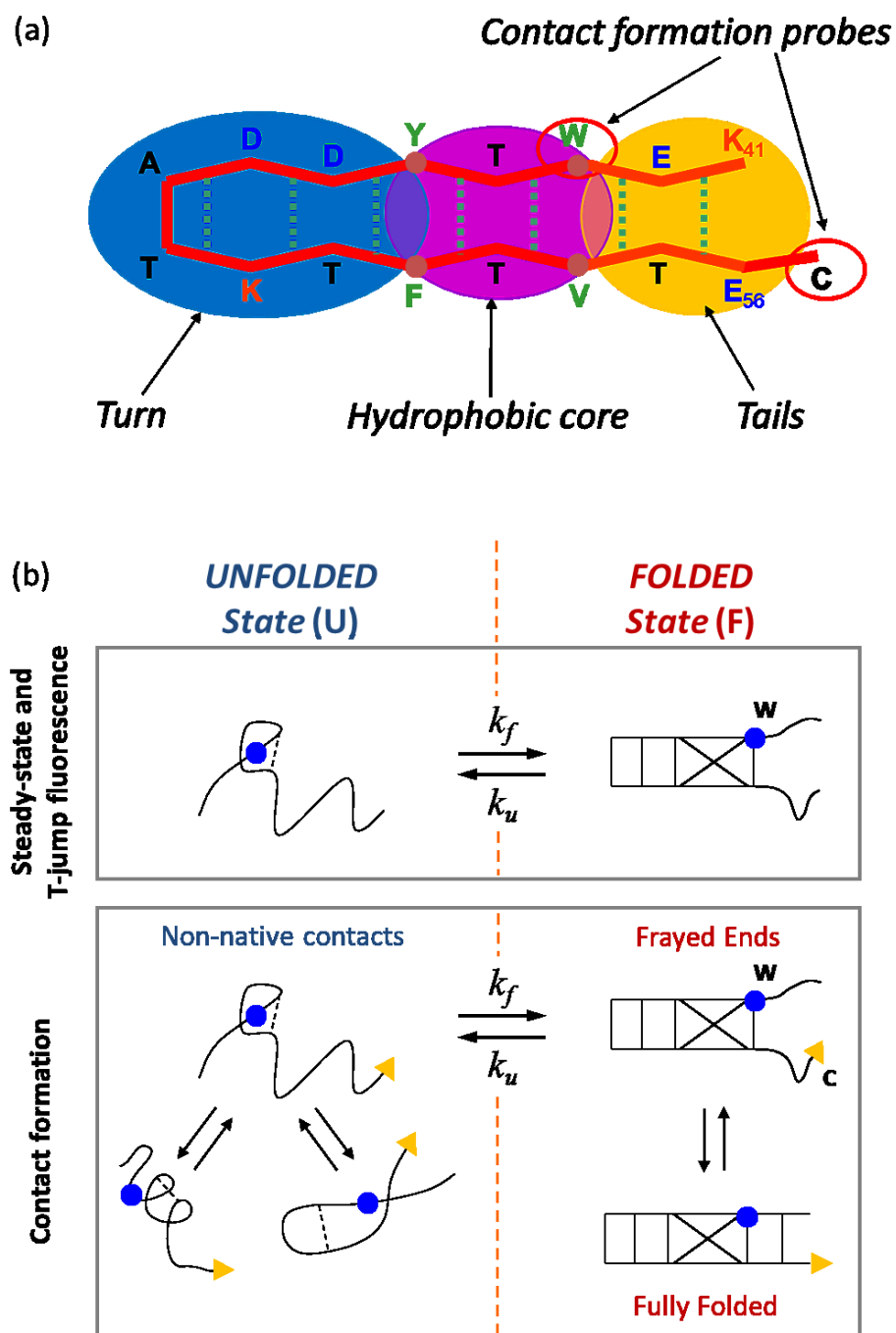


FIGURE 1

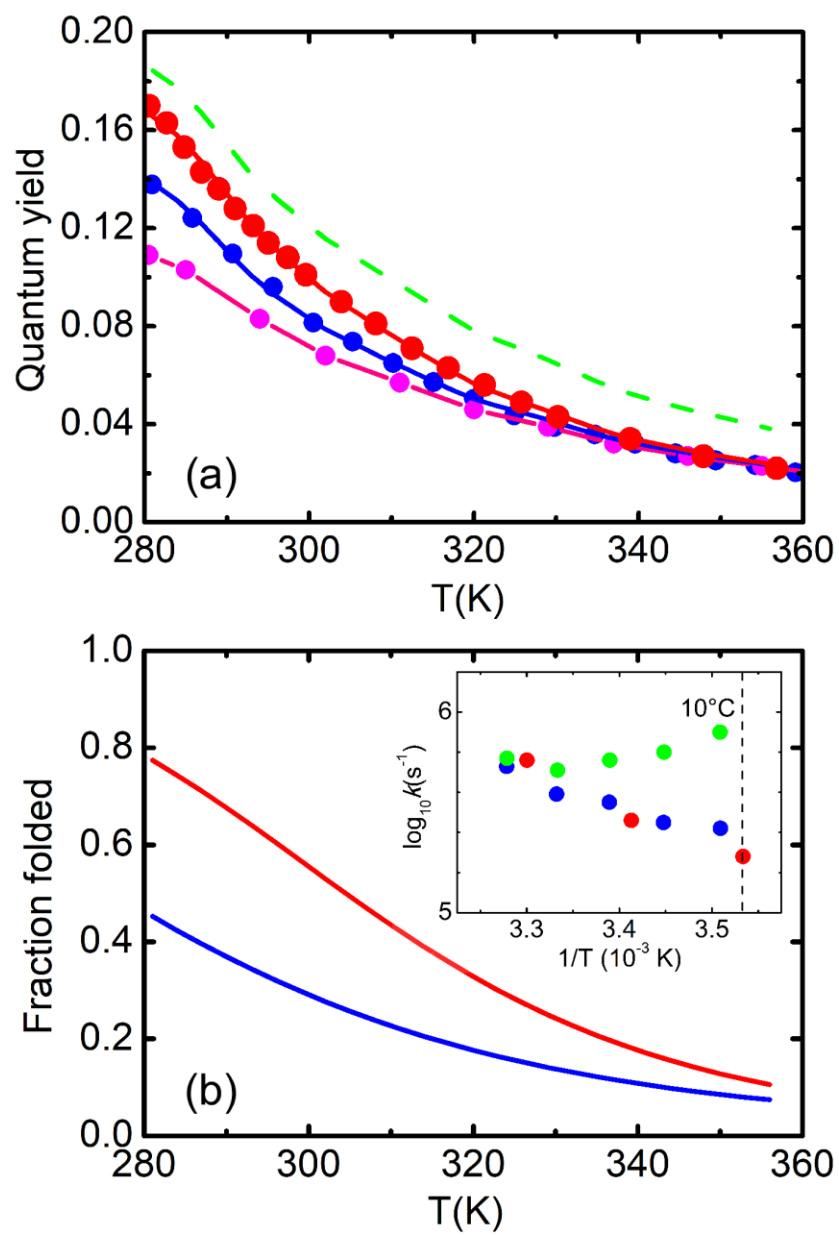


FIGURE 2

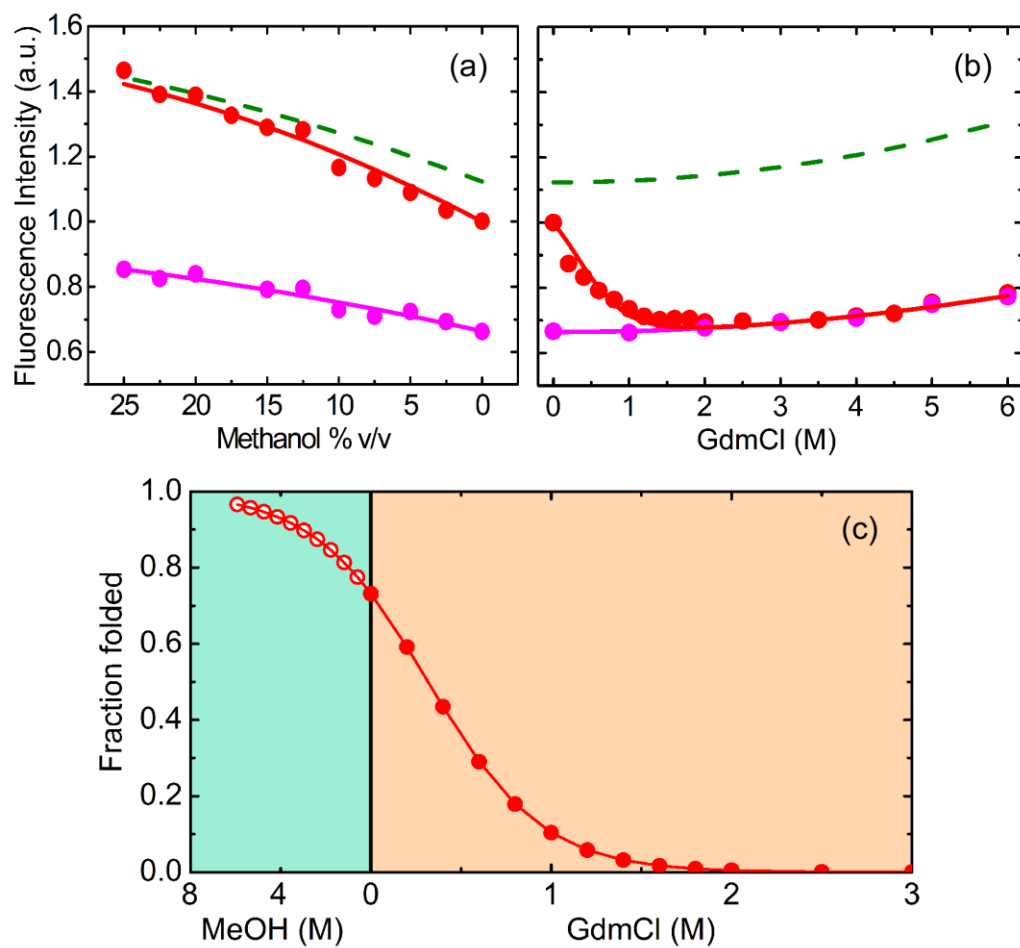


FIGURE 3

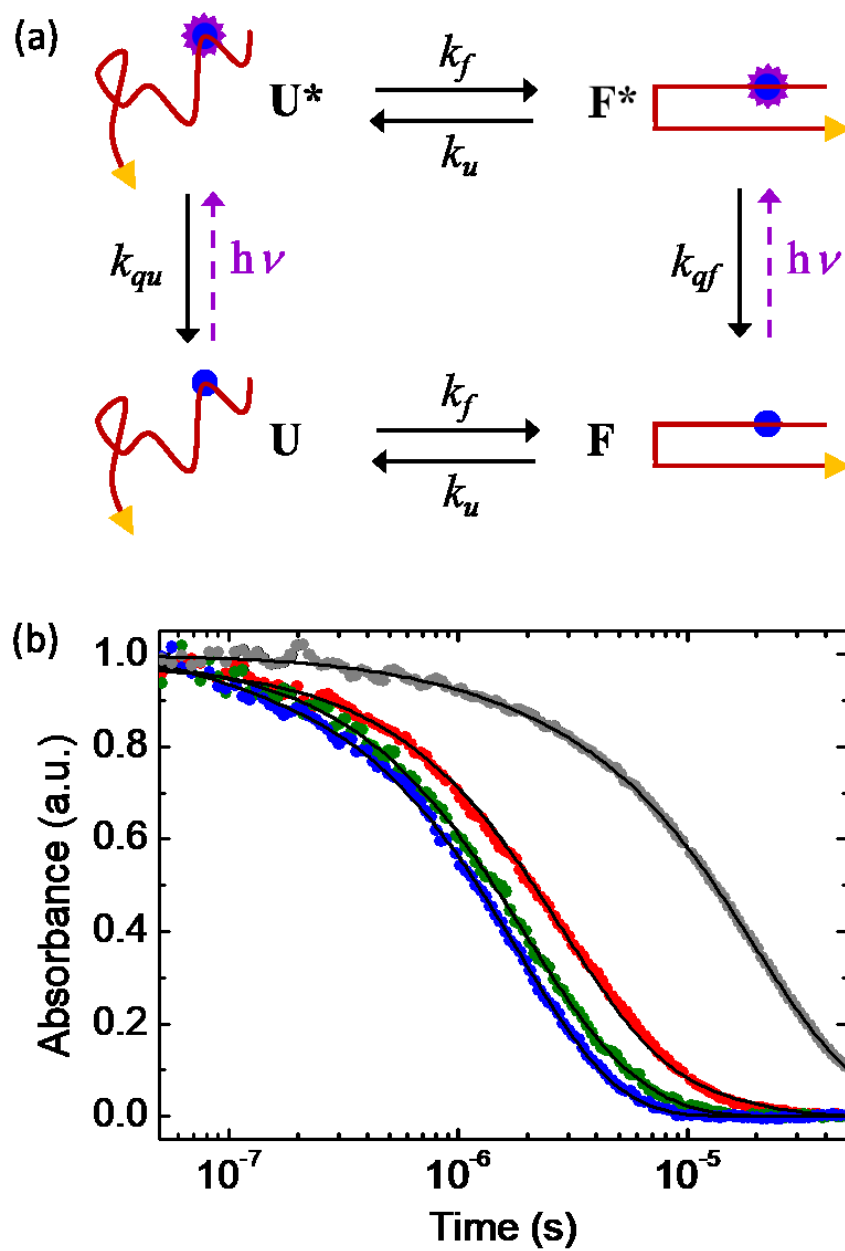


FIGURE 4

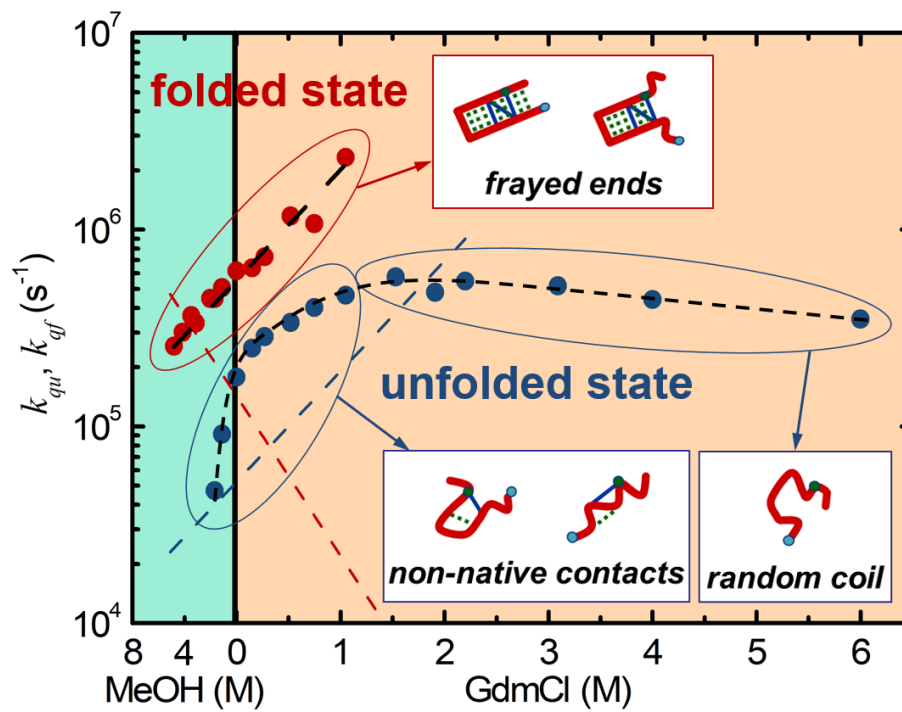


FIGURE 5

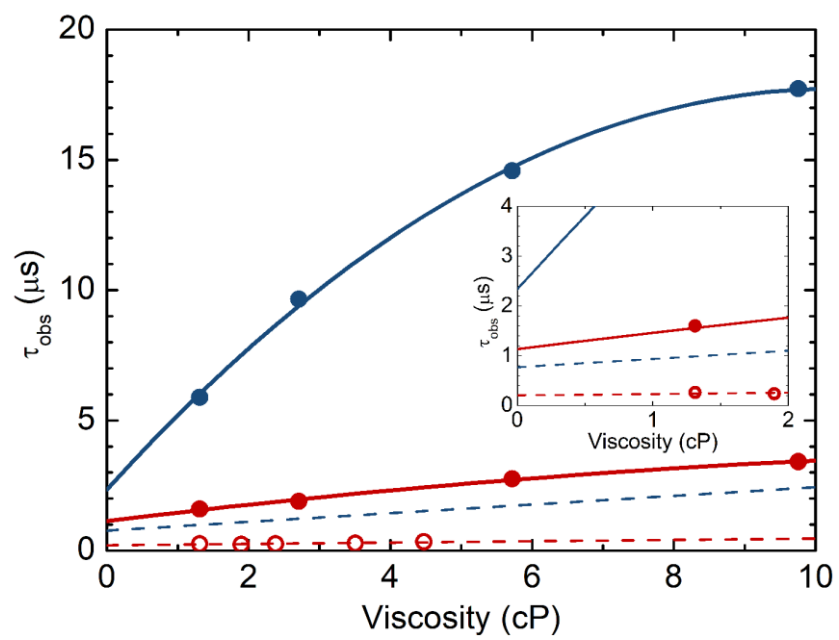


FIGURE 6

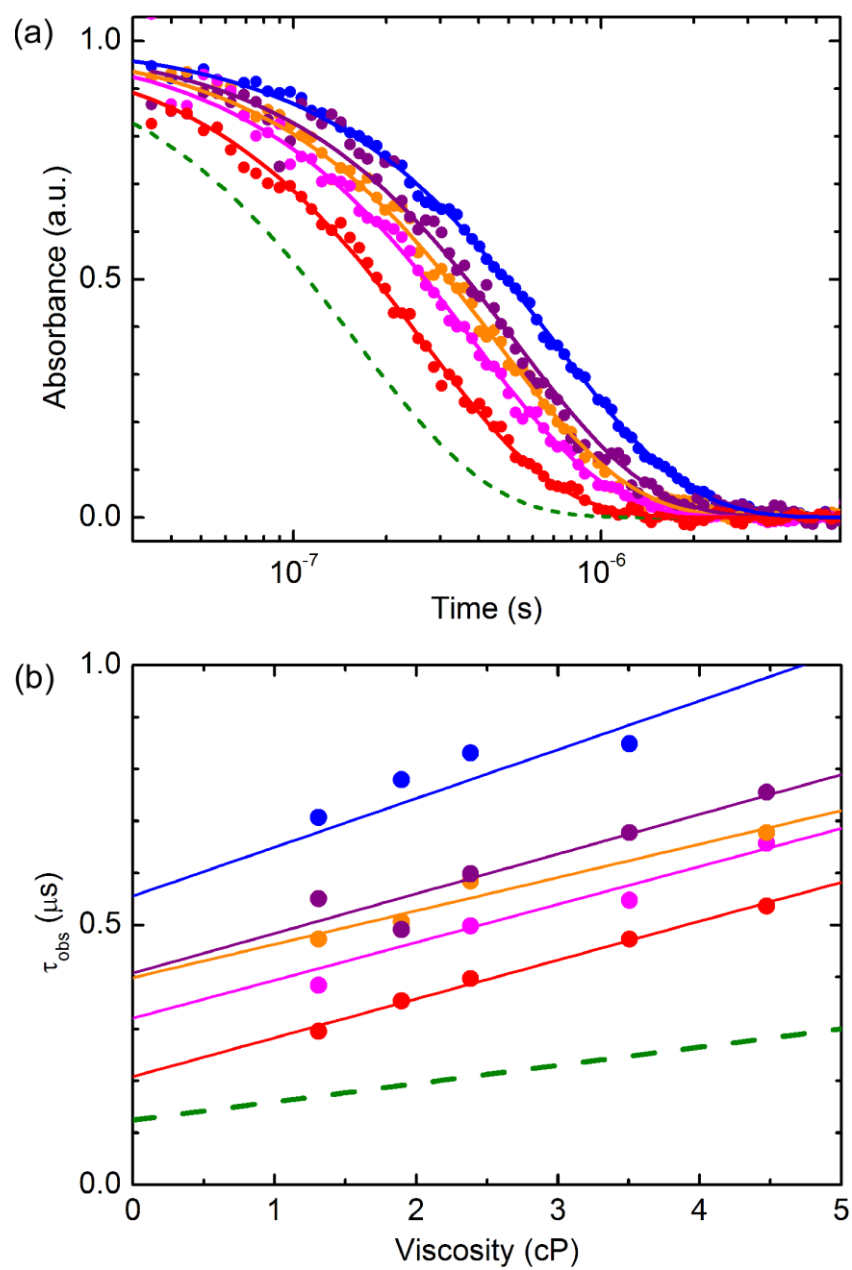


FIGURE 7

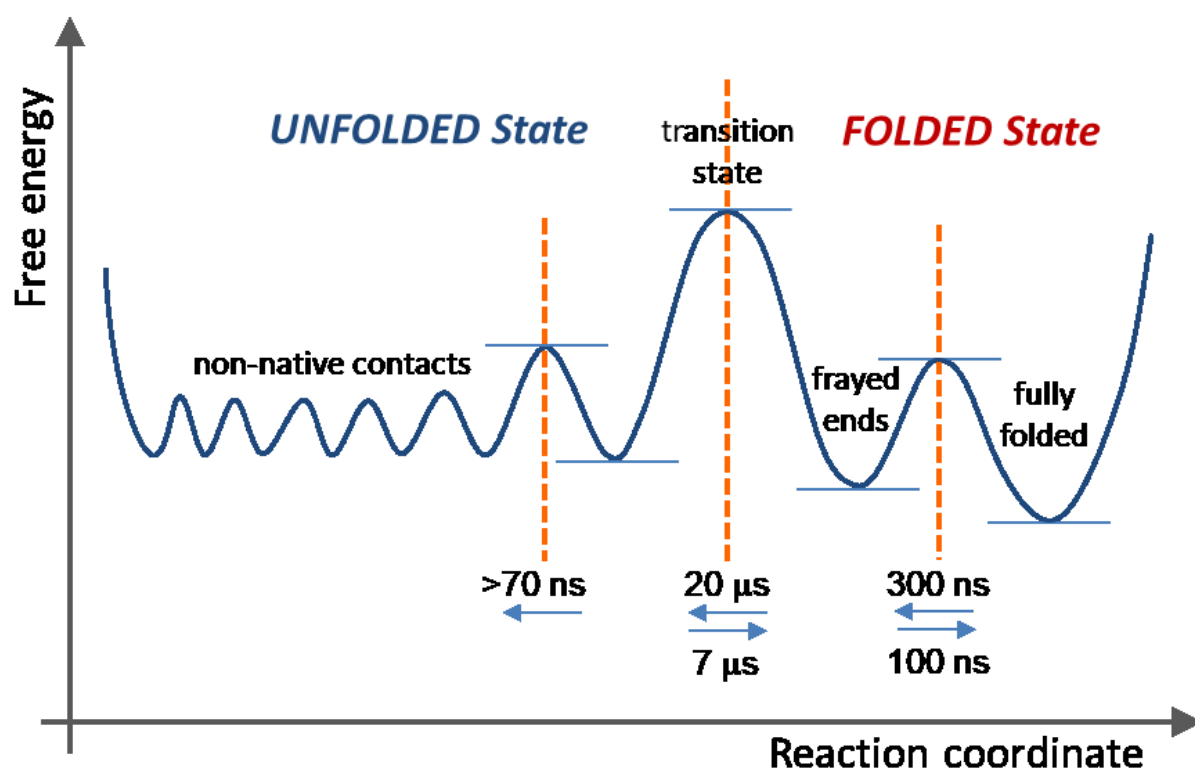


FIGURE 8



## TOC Graphic

